Obrabotka metallov -
Metal Working and Material Science

Journal homepage: http://journals.nstu.ru/obrabotka_metallov

Wear resistance and corrosion behavior of Cu-Ti coatings in SBF solution

Alexander Burkov [a], Maxim Dvornik [b], Maria Kulik [c, *], Alexandra Bytsura [d]

Khabarovsk Federal Research Center FEB RAS, 153 Tihookeanskaya st., Khabarovsk, 680042, Russian Federation

[a] https://orcid.org/0000-0002-5636-4669, ✉ burkovalex@mail.ru; [b] https://orcid.org/0000-0002-1216-4438, ✉ maxxxx80@mail.ru;
[c] https://orcid.org/0000-0002-4857-1887, ✉ marijka80@mail.ru; [d] https://orcid.org/0009-0005-4750-7970, ✉ alex_btsr@mail.ru

ARTICLE INFO

ABSTRACT

Introduction. Currently, titanium and its alloys have become the most popular metal implantable biomaterials. However, the main disadvantage of titanium alloys is low wear resistance due to high viscosity. It is known that copper-titanium coatings effectively improve the antibacterial properties of titanium alloy and at the same time increase its wear resistance. **Purpose of the work** is to study the effects of a solution simulating body fluid on corrosion properties, friction coefficient and the wear of copper-titanium coatings obtained by electrospark deposition method of the *Ti-6Al-4V* alloy. **Method.** A non-localized electrode consisting of copper and titanium granules in various ratios was used to form copper-titanium coatings on a titanium alloy by electrospark deposition. The structure of the coatings was examined using a *DRON-7* X-ray diffractometer in *Cu-Kα* radiation and an X-max 80 energy dispersive spectrometer. The antibacterial activity of the deposited *Cu-Ti* coatings was studied on a non-pathogenic gram-negative culture of *Escherichia coli*. Polarization tests in *SBF* solution were carried out using a *P-40X* potentiostat with an impedance measurement module. The metal content in the *SBF* solution after immersion of the samples was measured using an *ICP-MS 2000* mass spectrometer. The tribological characteristics of the coatings according to the *ASTM G99-17* standard using the "ball-on-disk" scheme with sliding friction in the *SBF* solution at loads of 10 and 25 N were examined. **Results and discussions.** It is shown that the bactericidal activity of *Cu-Ti* coated samples to a non-pathogenic culture of *Escherichia coli* increased monotonously with an increase in copper content. With copper concentration increasing, the corrosion current density of the coatings increased from 3.455 to 17.570 μA/cm^2. It is shown that the *SBF* solution accelerates the wear of a titanium alloy many times over due to its interaction with the electrolyte via the oxidative wear mechanism. The use of *Cu-Ti* coatings allows reducing the friction coefficient and greatly decreasing the wear of *Ti-6Al-4V* alloy in the presence of an electrolyte.

For citation: Burkov A.A., Dvornik M.A., Kulik M.A., Bytsura A.Yu. Wear resistance and corrosion behavior of Cu-Ti coatings in SBF solution. *Obrabotka metallov (tekhnologiya, oborudovanie, instrumenty) = Metal Working and Material Science*, 2024, vol. 26, no. 3, pp. 234–249. DOI: 10.17212/1994-6309-2024-26.3-234-249. (In Russian).

Introduction

Titanium and titanium alloys are used in many sectors of the national economy due to its outstanding mechanical properties (high strength, low density) and corrosion resistance [1]. Currently, titanium and its alloys have become more popular metal implantable biomaterials, compared to stainless steels and cobalt alloys, due to its better mechanical properties, high corrosion resistance and biocompatibility [2]. Titanium alloys are primarily used for orthopedic and dental implants. The failure rate of titanium implants is known to be 5–10 % over 15 years [3]. Bioinertness is one of the main reasons for poor osseointegration of titanium alloys. Therefore, for the successful use of titanium alloys in dentures or artificial joints, some obstacles still need to be overcome.

---

* Corresponding author
Kulik Maria A., Junior Researcher
Khabarovsk Federal Research Center FEB RAS,
153 Tihookeanskaya st.,
680042, Khabarovsk, Russian Federation
Tel.: +7 4212 22-69-56, **e-mail**: marijka@mail.ru

The main disadvantage of titanium alloys is low wear resistance, which leads to the release of wear products into the patient body. Another disadvantage of titanium is the lack of antibacterial properties, which can lead to infection or inflammation during clinical use and even to unsuccessful implantation [4, 5]. Antibacterial coating can reduce infections and inflammations caused by surgical contamination [6]. Copper-titanium coatings are known to effectively improve the antibacterial properties of titanium alloy and at the same time increase its wear resistance [7, 8]. *Cu-Ti* coatings are applied by magnetron sputtering [9–12], plasma spraying [6] and electrospark deposition (*ESD*) [13].

ESD is a high-energy process, the main advantages of which are the metallurgical bond of the formed coating to the substrate, the ability to select the coating thickness (from several units to several tens of micrometers), low thermal effect on the base material and simple equipment that does not require vacuum [14]. *ESD* technology is based on many low-voltage electrical discharges passing between the electrode and the workpiece in a gas environment. During the discharge, a microbath of molten metal on the cathode surface is formed, into which the material is transferred from the anode, the so-called polar transfer. As a result of convective and diffusion mixing of the anode and cathode materials, high adhesion of the coating to the substrate is provided. Due to the short discharge lifetime $\leq 10^{-4}$ s the low thermal effect on the substrate is ensured [15, 16]. In this work, a non-localized electrode was used, which ensured automation of *ESD* processing. The concept of a non-localized electrode is based on the use of a set of millimeter-sized granules as a source of deposited material [17–19]. Previously, we deposited *Cu-Ti* coatings by the method of electrospark deposition (*EGD*) using a non-localized electrode [20, 21] and studied its wear behavior under dry sliding conditions. However, there is no information in the literature on the corrosion and tribological behavior of copper-titanium coatings in physiological solutions, despite the fact that a significant effect of electrolytes on the friction coefficient, wear mechanism of materials and corrosion properties is known. The purpose of the work is to study the effects of a solution simulating body fluid (*SBF*) on corrosion properties, friction coefficient and the wear rate of copper-titanium coatings obtained by electrospark deposition method of the *Ti-6Al-4V* alloy.

Research methodology

Copper-titanium coatings were prepared by the *EGD* method using a non-localized electrode (*NE*) as an anode. It consisted of a set of cylindrical granules ($d = 4 \pm 0.5$ mm, $h = 4 \pm 1$ mm) of titanium *VT1-00* and copper *M0*. The composition of five *NEs* with different ratios of titanium and copper granules is presented in Table 1. Cylinders ($h = 10$ mm, $d = 12$ mm) made of industrial titanium alloy *Ti-6Al-4V* were used as a substrate (cathode). Before applying the coatings, the substrates were processed on *P600* abrasive paper, then alternately washed in water and alcohol using an ultrasonic bath and dried in a drying oven at 90 °C. The sets of granules were poured into a titanium container, in the center of which the substrate was placed. The substrate and container were connected to the negative and positive leads of the pulse generator, respectively. The substrate and container with granules were rotated in opposite directions with a frequency of 60 rpm using motors.

The pulse generator operating parameters were as follows: pulse duration 100 μs, repetition frequency 1 kHz, voltage 30 V, current pulse amplitude 110 A. Surface oxidation and nitriding during coating application were eliminated by feeding argon into space of the container with granules. Each set of granules was run in on a non-replaceable cathode for ~2 hours. The processing of one sample lasted 10 minutes. The method of deposition of *Cu-Ti* coatings is described in detail in [19–21].

T a b l e 1

Composition of a set of granules for coating

Sample designation	*Cu10*	*Cu30*	*Cu50*	*Cu70*	*Cu90*
Cu, at. %	10	30	50	70	90
Ti, at. %	90	70	50	30	10

X-ray analysis of the samples was performed on a *DRON-7* X-ray diffractometer at a scanning rate of $0.05°s^{-1}$ using a copper tube. The antibacterial activity of the deposited *Cu-Ti* coatings was studied on a non-pathogenic gram-negative culture of *Escherichia coli* cultivated on meat-peptone agar (*MPA*). Test samples were placed in sterile *Petri* dishes ($d = 100$ mm). 0.04 ml of the cultured culture with a concentration of 10^5 COE/ml was dropped onto the surface of each sample. The samples were incubated for 24 hours at a relative humidity of ≥ 90 %, the temperature was maintained at 36 °C. Then, bacteria were washed off the surface of the samples with a phosphate buffer solution (1.6 ml). To count the colonies of surviving bacteria, suspensions were obtained, which were then applied to a *Petri* dish with *MPA* and incubated for 24 hours at a temperature of ~ 36 °C. Corrosion and tribological tests were carried out in an *SBF* solution (Table 2), the composition of which is close to human blood plasma [22]. Polarization tests were carried out using a *P-40X* potentiostat equipped with an impedance measurement module (Electro Chemical Instruments, Russia). The reference electrode was an *Ag*/*AgCl* electrode, the auxiliary electrode was an *ETP-02* platinum electrode, and the working electrode was titanium sample with coating. The sample exposure area was 1 cm^2. The scanning rate in the range of -0.8–0 V was 4 mVs^{-1}. The concentration of metals in the *SBF* solution after immersion of the samples was measured using a mass spectrometer with inductively coupled plasma (*ICP-MS 2000*). *Cu-Ti* coating samples with an exposed surface area of 2.88 cm^2 were immersed in 50 ml of *SBF* solution at room temperature for 24 h.

T a b l e 2

Ion concentration in *SBF* solution

Ions	HPO_4^{2-}	Mg^{2+}	Ca^{2+}	HCO^{3-}	K^+	Na^+	Cl^-
Concentration, mg/l	1.00	1.50	2.50	4.20	5.00	14.00	148.80

Tribological tests were carried out according to the *ASTM G99 – 17* standard using the "ball on disk" scheme with sliding friction in *SBF* solution; a disk made of high-speed steel *M45* was used as a counterbody at a rotation speed of 3 rpm, with a sliding circle diameter of 5 cm, under loads of 10 and 25 N. A peristaltic pump supplied *SBF* solution to the friction zone at a rate of 1 ml·min^{-1}. For each sample, 5 measurements of the friction coefficient and wear rate were made. The microstructure of the surface of worn coatings was studied using a *Vega 3 LMH* scanning electron microscope (*SEM*). An *X-max 80* energy dispersive spectrometer (*EDS*) (Oxford Instruments, UK) was used for microanalysis of the surface of samples after wear testing.

Results and its discussion

Under the influence of electric discharges occuring between copper and titanium granules, its surface layers melt and intensive exchange of material occurs between it. Preliminary running-in of *NE* leads to the formation of a secondary structure on the surface of all granules, represented by a copper-titanium layer similar to the coating on the substrate. During the *EGD* treatment of samples, discharges occur between the granule and the substrate and the copper-titanium composition of the secondary structure of the granule is transferred to substrate surface, and not pure copper or titanium, as in the case of traditional *ESD* processing of titanium alloy with a copper electrode or vice versa. In addition, unlike traditional *ESD*, when using *NE*, the formed *Cu-Ti* erosion particles remain in the system and can re-participate in the process of coating formation.

When an electric discharge passes between the granule and the substrate, a melt microbath is formed on the cathode, into which the molten granule material is transferred and mixed with the substrate material. During the discharge, a dynamic equilibrium on the cathode is formed, in which more material enters to melt microbath than leaves it as erosion result. After the discharge is complete, the microbath material
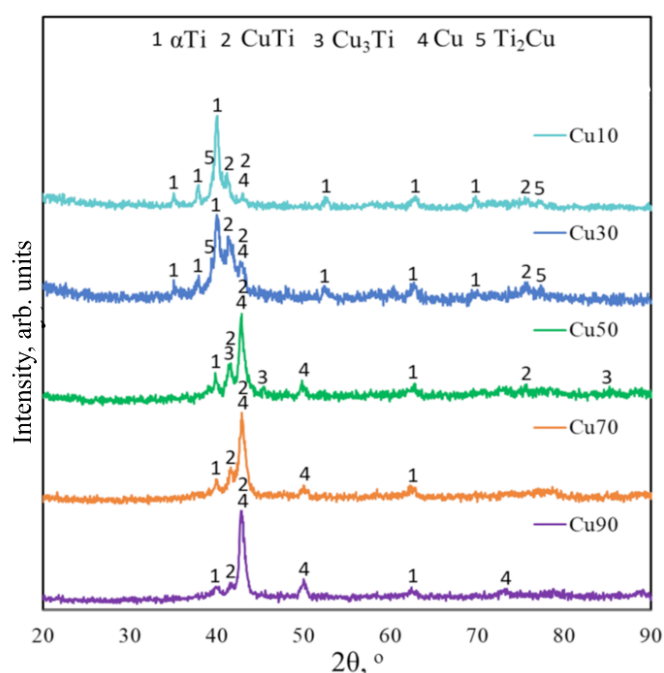
Table 3

Thickness and roughness of *Cu-Ti* coatings

Parameters	Samples				
	Cu10	*Cu30*	*Cu50*	*Cu70*	*Cu90*
Average thickness, μm	32.3 ± 9.9	32.4 ± 7.4	43.7 ± 9.4	49.3 ± 8.3	45.2 ± 13.2
Roughness, *Ra*, μm	6.3 ± 1.4	6.8 ± 1.6	6.9 ± 0.9	7.3 ± 1.1	7.5 ± 1.1

crystallizes, forming a coating. Thus, the thickness of the formed *ESD* coating is determined by the depth of the melt microbath on the cathode at the end of the discharge [23]. The average thickness of the deposited *Cu-Ti* coatings ranged from 32.3 to 49.3 μm (Table 3). The dependence of the average coating thickness on the copper concentration in the *NE* had the parabolic form with a maximum for the *Cu70* sample. This can be explained by the proximity of this copper to titanium ratio to the eutectic point of the *Cu-Ti* phase diagram; the secondary structure on the surface of the *NE* granules for the *Cu70* samples had the lowest melting temperature [24].

Fig. 1 shows sections of X-ray diffraction patterns of copper-titanium coatings. The obtained coatings contain copper, *αTi*, and intermetallics: Ti_2Cu, *CuTi*, and Cu_3Ti. With an increase in the proportion of copper granules in the *NE*, the deposited coatings were enriched with copper and copper-rich intermetallics. The *CuTi* phase is observed in all coatings. It was also observed in studies on magnetron sputtering [12]. It is known that the hardest phase is Ti_2Cu (746.9 ± 67.7 HV), while the *CuTi* phase is much softer (298.2 ± 20.7 HV) [25]. The hardness of the copper-rich phase Cu_3Ti occupies an intermediate position; its hardness is 544.34 HV [26]. In the composition of copper-rich samples (*Cu70* and *Cu90*), the metallic copper phase predominated. Thus, by changing the ratio of copper and titanium granules in the *NE*, it is possible to vary the phase composition of the deposited coatings.

Fig. 2 shows the potentiodynamic polarization curves of the *Ti-6Al-4V* alloy with and without *Cu-Ti* coatings in the *SBF* solution at room temperature. The *Tafel* slopes of the polarization curves were used to calculate the corrosion potential (E_{corr}) and corrosion current density (I_{corr}), which are presented in Table 4. The results show that E_{corr} is decreased with an increase in the copper content in the coating. It was found

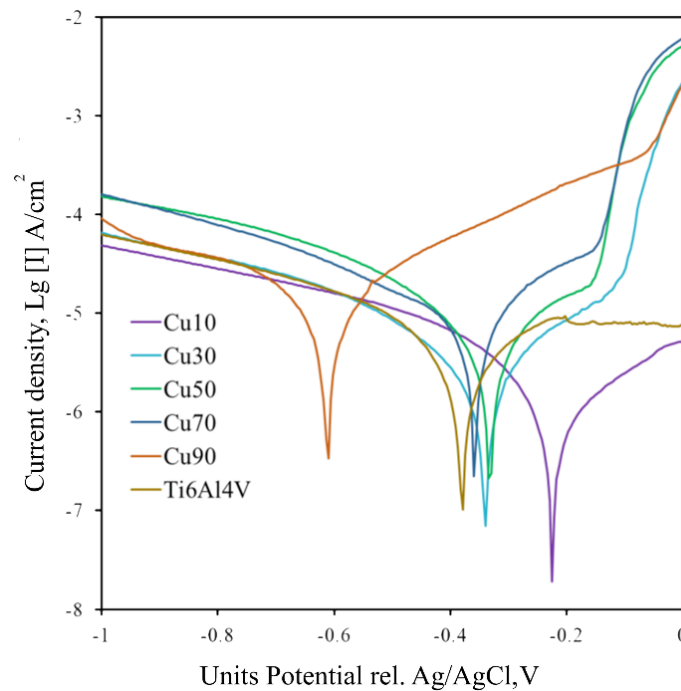*Fig. 1*. Results of X-ray analysis of *Cu-Ti* coatings

Fig. 2. Polarization plots of *Cu-Ti* coatings
and *Ti-6Al-4V* alloy in *SBF* solution

Table 4

Copper concentration in the composition of *Cu-Ti* coatings and its corrosion parameters in *SBF* solution

Parameter	Samples					
	Ti-6Al-4V	*Cu10*	*Cu30*	*Cu50*	*Cu70*	*Cu90*
E_{corr}, V	−0.38	−0.23	−0.34	−0.33	−0.36	−0.61
I_{corr}, μA/cm^2	9.00	3.46	7.05	8.75	8.45	17.57
Copper concentration, at.%	–	12.5	24.3	36.8	61.4	74.1

that the *Cu10–Cu70* coatings have a higher corrosion potential than the substrate, i.e. these coatings are more noble. Because of this, a galvanic couple can be formed between the coating and the substrate, where the substrate will undergo anodic corrosion. The corrosion current density determines the corrosion rate of the material. With an increase in the titanium concentration in the coatings, I_{corr} decreased from 17.570 to 3.455 μA/cm^2. It was shown that for all coatings except *Cu90*, I_{corr} was lower than that of the *Ti-6Al-4V* alloy. Thus, polarization tests indicate an increase in the corrosion resistance of the *Ti-6Al-4V* alloy when using *ESD Cu-Ti* coatings with a copper content of less than 70 at. %. The corrosion resistance of *Cu-Ti* compositions is usually associated with the passivation film of Cu_2O, which is resistant to the effects of Cl^- ions due to the formation of insoluble copper (I) chloride [27].

For a more detailed research of the corrosion characteristics for all samples, electrochemical impedance spectroscopy (*EIS*) was used, which can be classified as a non-destructive testing method due to the low voltage and low current flowing through the sample [28]. Fig. 3 shows the experimental results on *EIS*. As a rule, the capacitive arc on the *Nyquist* plot is explained by charge transfer reactions occurring at the metal/solution interface or associated with the features of the surface passive layer. It is known that with an increase in the radius of the capacitive arc, charge transfer is hindered, which has a positive effect on the corrosion resistance of the material [29]. The radius of the capacitive arc of the samples increased in the series: *Cu90*, *Cu70*, *Cu50*, *Cu30*, *Cu10* (Fig. 3 *a*, *b*). That is, charge transfer became more difficult
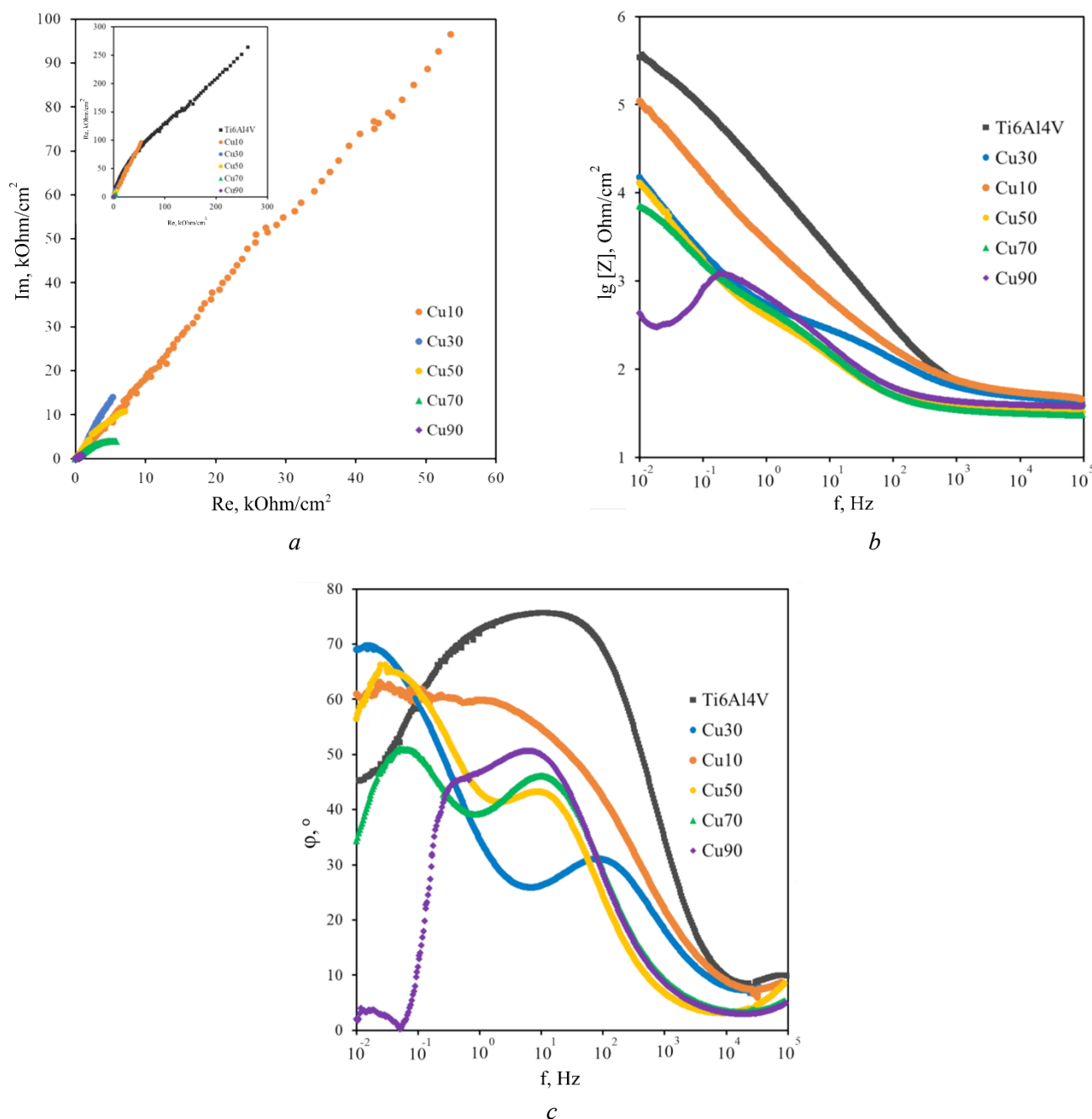
a

b

c

Fig. 3. Impedance plots of *Cu-Ti* coatings in *Nyquist* coordinates (*a*), total *Bode* impedance (*b*) and phase angle (*c*)

monotonically with a decrease in the copper concentration in the *Cu-Ti* coatings. At the same time, all samples with *Cu-Ti* coatings had a smaller radius of the capacitive arc than the untreated substrate. As follows from the *Bode* impedance diagram, the spectrum of the *Ti-6Al-4V* alloy in the mid-frequency range (10^{-1}–10^3 Hz) has a wide linear region, which indicates the formation of a single-layer passive layer in the *SBF* solution (Fig. 3 *b*). In the coatings, the linear region narrowed with increasing copper concentration, which indicates the formation of additional passive layers. It is shown that with an increase in the copper concentration in the *NE*, the capacitance of the barrier layer on the coating surface decreases, as indicated by a decrease in the slope of the corresponding curves in the logarithmic coordinates. It is known that, in the general case, the anticorrosive properties of the material are in direct proportion to the resistance of the barrier layer and inversely dependent on its capacitance [30]. The compactness of the formed oxide film is determined by the convexity magnitude in the mid-frequency range on the *Bode* phase angle graph (Fig. 3 *c*). For the *Ti-6Al-4V* alloy, the convexity value was higher than 75°. It is known that the phase angle

value for an ideal capacitor is 90°. At this phase angle value, there is an ideally dense oxide film on the surface that can effectively inhibit charge transfer processes [31]. For all samples with copper-titanium coatings, the largest phase angle values were lower than 60°. This indicates that the oxide film formed on the surface of copper-titanium coatings was looser compared to the titanium alloy. Moreover, the coatings have two convexity maxima, which indicate a more complex oxide film compared to the titanium alloy. Comparing the convexity width on the phase angle graphs, it can be concluded that it decreases monotonically with increasing copper concentration in the coatings. Thus, the stability of the oxide film formed on the samples decreased with decreasing titanium concentration. In general, the results of impedance spectroscopy are in good agreement with the polarization data of the samples (Table 4). Thus, in the *SBF* solution, copper-titanium coatings *Cu10–Cu70* have better corrosion resistance compared to the titanium alloy, but the barrier films formed on it are more permeable than on the *Ti-6Al-4V* alloy.

Table 5 shows the concentration of dissolved copper ions after immersion of *Cu-Ti* coated samples in *SBF* solution for 24 h. It can be found that the concentration of copper ions was in the range of 98.6 to 484.9 µg/L; the minimum concentration was characteristic of *Cu50* sample, and the maximum concentration was characteristic of *Cu70* sample. According to the works on copper-titanium alloy (*Ti* – 5 wt. % *Cu*), the release of copper ions into 0.9 wt. % *NaCl* solution after anodizing was in the range of 52 to 239 µg/L [32], and after acid etching it was in the range of 26 to 386.9 µg/L [33], despite the fact that the copper concentration in the alloy was several times less than in the case of our coatings. The safe concentration of copper in drinking water, according to the World Health Organization, is < 2 mg/L [34]. Thus, the copper concentration released into the *SBF* solution from the developed *Cu-Ti* coatings is many times lower than the permissible values and therefore it can be used as biocompatible coatings. Another significant element is aluminum, which is released from the *Ti-6Al-4V* alloy and accumulates in the body of patients with implants. Despite the low concentration of aluminum in the *Ti-6Al-4V* alloy (~ 6 wt. %), it was released from the surface of the samples in quantities comparable to copper.

Table 5

Content of metals released from the samples into the *SBF* solution

Samples	Concentration of metals, µg/dm^3			
	Al	*Ti*	*V*	*Cu*
Cu10	188.45	1.67	6.15	193.98
Cu30	57.98	3.71	4.39	243.50
Cu50	54.14	1.17	6.82	98.55
Cu70	198.02	0.90	3.88	484.92
Cu90	98.37	5.17	4.69	145.15

The antibacterial activity (*AA*) of the samples with copper-titanium coatings was calculated using the method [35] in accordance with expression (1):

$$AA = \frac{(A - B) \times 100}{A},$$ (1)

where: *A* is the number of bacterial colonies in the *Petri* dish for the reference metal; *B* is the number of bacterial colonies in the dish for the bactericidal metal.

According to the calculations, the antibacterial activity of *Cu-Ti* coatings to the culture of non-pathogenic *Escherichia coli* monotonously increased from 25.5 ± 4.2 to 62.8 ± 5.4 % (Fig. 4). In real conditions of use, a longer contact (> 24 h) of the environment with the surface of copper-titanium coatings will lead to its complete disinfection. The result of the experiment showed that all deposited *Cu-Ti* coatings exhibited bactericidal activity. The highest concentration of copper in the *Cu90* sample resulted in the
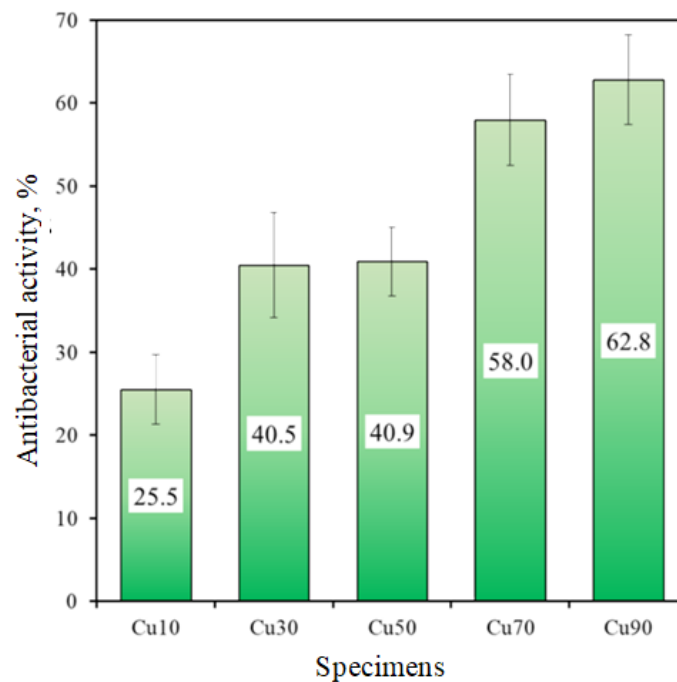
Fig. 4. Antibacterial activity (*AA*)

highest bactericidal activity. The *Cu50* sample is the most optimal in terms of low concentration of released copper ions and sufficient antibacterial activity.

The results of tribological tests of copper-titanium coatings in comparison with *Ti-6Al-4V* alloy in *SBF* solution at normal loads of 10 and 25 N are shown in Figure 5. It was found that with an increase in the applied load from 10 to 25 N, the average values of the friction coefficient (*COF*) of the titanium alloy *Ti-6Al-4V* decreased from 0.45 to 0.36 (Fig. 5 *a*). Similarly, the friction force during the wear of *Cu-Ti* coatings decreased with an increase in the specific load. Thus, the average *COF* values of *Cu-Ti* coatings at load of 10 N were in the range from 0.39 to 0.55, while at 25 N it was in the range from 0.28 to 0.40 (Table 6). This leads to the conclusion that part of the applied load is compensated by the pressure of the oncoming liquid flow. The highest values of *COF* at both loads were observed for the *Cu70* sample, while the lowest values of *COF* were for *Cu50 sample*. The use of the latter allows reducing the friction force of the *Ti-6Al-4V* alloy by 14–21 %. Previously, at a load of 25 N, we found that *COF* of copper-titanium coatings without *SBF* was much higher and was in the range from 0.73 to 0.96. Moreover, *COF* of the coatings under dry friction was significantly higher than that of the *Ti-6Al-4V* alloy [19].

Fig. 5 *b* shows the diagrams of wear rate values of titanium alloy samples with copper-titanium coatings in *SBF* solution. The wear rate of samples with *Cu-Ti* coatings was within the range from 0.71×10^{-5} to 2.70×10^{-5} mm^3/Nm under a load of 10 N and from 0.70×10^{-5} to 1.79×10^{-5} mm^3/Nm under a load of 25 N. Under both loads, the *Cu50* coating had the highest wear resistance, which is explained by its lowest friction coefficient. Under a load of 10 N, the wear rate of the *Ti-6Al-4V* alloy in *SBF* solution was 3.58×10^{-4} mm^3/Nm, and under 25 N it was 3.99×10^{-4} mm^3/Nm. Thus, the wear resistance of the alloy was 13 to 57 times lower than that of the coatings. It is characteristic that the wear of the *Ti-6Al-4V* alloy under dry sliding conditions at 25 N was 0.75×10^{-4} mm^3/Nm [20], which is 5.3 times lower than that in the *SBF* solution, which is consistent with the results of work [36]. Thus, the *SBF* solution repeatedly accelerates the wear of the titanium alloy due to its interaction with the electrolyte according to the oxidative wear mechanism [36]. Oxidative products, and primarily rutile, can act as abrasive particles, accelerating the wear of the titanium alloy. Comparison of the wear intensity of *Cu-Ti* coatings under a load of 25 N showed that most of the samples also had increased wear in the *SBF* solution compared to the dry sliding mode, with the exception of the *Cu50* and *Cu70* coatings, which had very close wear values in *SBF* and dry environments. Thus, the use of *Cu-Ti* coatings for products made of titanium alloy *Ti-6Al-4V* allows reducing its wear many times over and lowering the coefficient of friction when used in *SBF* solution.
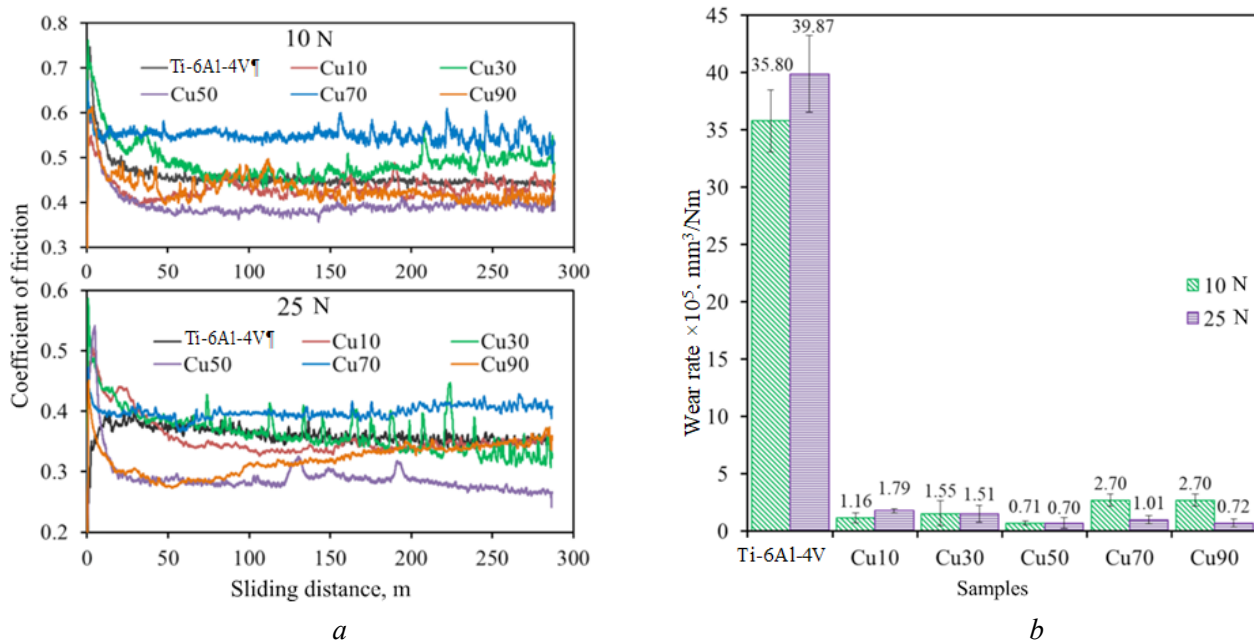
Fig. 5. Friction coefficient (*a*) and wear rate (*b*) of *Cu-Ti* coatings and *Ti-6Al-4V* alloy in *SBF* solution under various loads

Table 6

Averaged *COF* values of samples with coatings in *SBF* solution

Load, N	Samples					
	Ti-6Al-4V	*Cu10*	*Cu30*	*Cu50*	*Cu70*	*Cu90*
10	0.449	0.430	0.480	0.387	0.548	0.425
25	0.361	0.346	0.358	0.284	0.399	0.320

Figure 6 shows *SEM* images of wear track of *Cu-Ti* coatings after tribological testing in *SBF* solution. It shows that on the worn surface of the *Ti-6Al-4V* alloy, as a result of plowing up, were formed tracks that look like wide grooves and scratches, which indicate abrasive wear. At the same time, there are signs of adhesive wear, such as areas with delamination and strong deformation. The images clearly show that the worn surface of the *Ti-6Al-4V* alloy is rougher, and the surface of the *Cu-Ti* coatings is smoother. The smoothest surface was observed in the case of the *Cu50* sample (Fig. 6 *c*), and the most relief one was observed in the case of the least wear-resistant *Cu90* coating (Fig. 6 *e*). In contrast to dry friction in the *SBF* solution, no oxide wear flakes were observed on the surface of the coatings. This indicates that, during friction in liquid, the oxidative products are actively removed from the friction zone. Therefore the protective tribooxide layer is not preserved, which is expressed in increased wear rate values, compared to dry friction. Wear products were preserved only in surface depressions such as pores and cracks. According to the results of *EDS* analysis, the wear products contain iron, tungsten and chromium, which were deposited on the coating surface as a result of intensive wear of the counterbody made of high-speed steel *M45* (Table 7). A significant amount of oxygen indicates oxide accumulations, which is a consequence of oxidative wear [37]. The presence of *Cl*, *S* and *P* elements is explained by the participation of the *SBF* solution in the formation of wear products. The oxygen concentration decreased in the wear products with an increase in the copper content in the coatings, which is explained by a higher standard electrode potential of copper compared to titanium. Thus, the main wear mechanism of copper-titanium coatings was a combination of oxidation and abrasive wear, while for titanium alloy the adhesive wear mechanism was more typical.
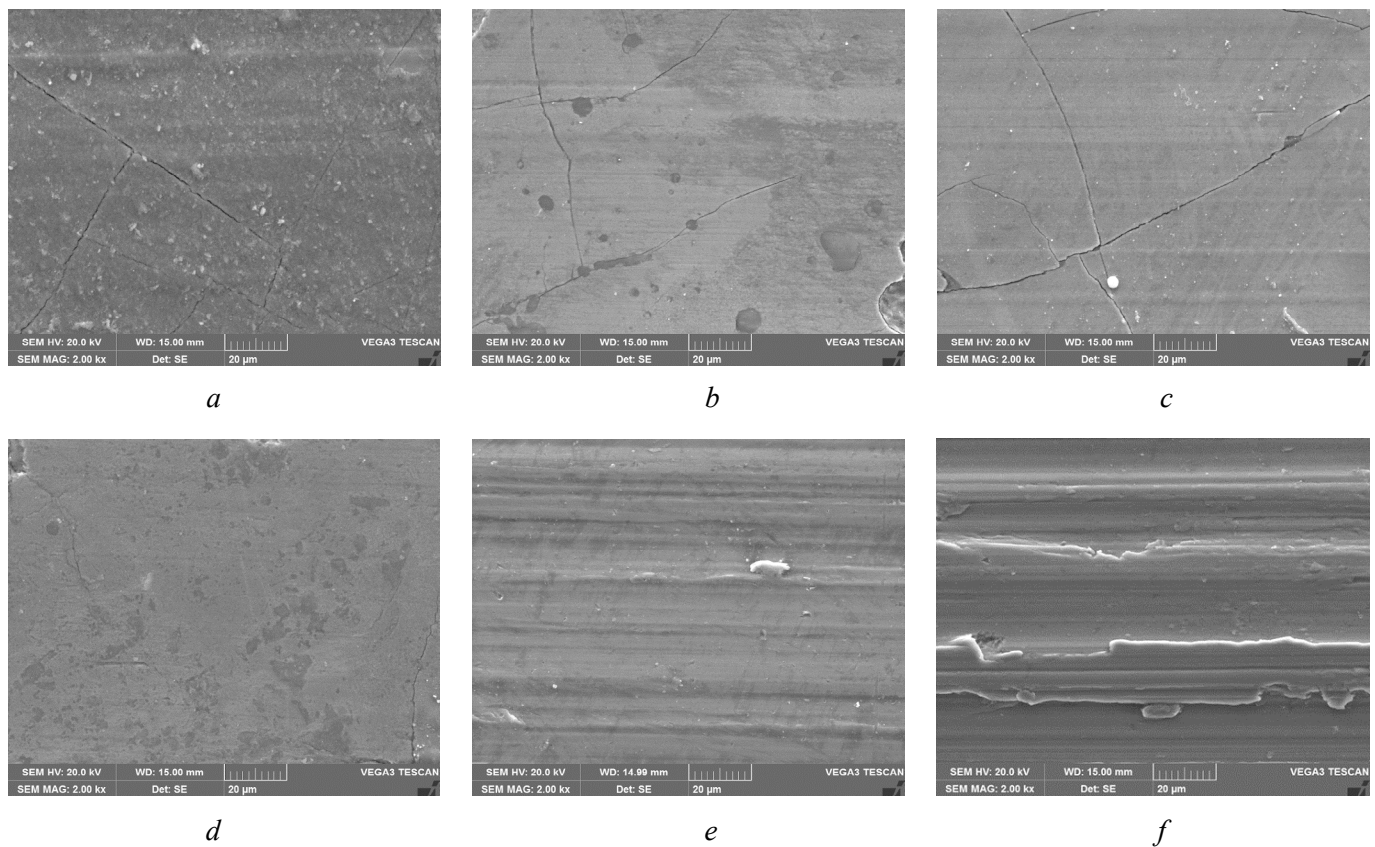
Fig. 6. SEM photos of the worn surface of *Cu-Ti* coatings after wear testing in *SBF* solution:
a – Cu10; *b – Cu30; c – Cu50; d – Cu70; e – Cu90; f – Ti-6Al-4V*

T a b l e 7

Composition of wear products on the surfaces of coatings and *Ti-6Al-4V* alloy

Element	Concentration, at.%					
	Cu10	*Cu30*	*Cu50*	*Cu70*	*Cu90*	*Ti-6Al-4V*
C	25.38	5.67	22.72	13.08	16.71	7.16
O	53.95	63.5	50.1	43.3	42.68	20.09
Al		0.47		0.19	0.33	4.37
P	0.07		0.07		0.08	
S	0.1	0.19	0.12		0.14	0.11
Cl	0.22	0.59	0.41	0.18	0.35	0.32
Ti	1.59	12.28	11.99	37.90	26.03	63.87
V		0.53		0.87		3.2
Cr	0.22	0.7	0.4	0.16	0.37	
Fe	18.02	12.61	8.43	0.39	9.86	0.88
Cu	0.38	3.02	5.62	3.93	3.24	
W	0.07	0.44	0.14		0.22	

Conclusions

Copper-titanium coatings on titanium alloy blanks were prepared by the method of electric spark deposition using a non-localized electrode consisting of copper and titanium granules in different ratios. The copper concentration in the coatings monotonically increased with its content in the electrode. It is shown

that with an increase in the copper concentration, the corrosion current density of the coatings increased from 3.455 to 17.570 µA/cm^2. It is found that in the *SBF* solution, copper-titanium coatings *Cu10–Cu70* have a higher corrosion potential and better corrosion resistance compared to the *Ti-6Al-4V* alloy, but the passivation films formed on it are more permeable than on the *Ti-6Al-4V* alloy. All compositions of the *Cu-Ti* coatings showed bactericidal activity towards the non-pathogenic culture of *Escherichia coli*. It is shown that the electrospark deposition of *Cu-Ti* coatings reduces the surface wear of the titanium alloy *Ti-6Al-4V* in *SBF* solution many times over. Despite the lubricating effect, the wear in the *SBF* solution is more severe for the *Ti-6Al-4V* alloy and copper-titanium coatings compared to wear under dry friction conditions due to the intensive removal of the antifriction tribooxide layer. The combined action of abrasive wear and oxidation accelerated by the electrolyte was the main wear mechanism of the copper-titanium coatings, while for the *Ti-6Al-4V* alloy, adhesive wear was more characteristic.

References

1. Geetha M., Singh A., Asokamani R., Gogia A. Ti based biomaterials, the ultimate choice for orthopaedic implants – a review. *Progress in Materials Science*, 2009, vol. 54, pp. 397–425. DOI: 10.1016/j.pmatsci.2008.06.004.

2. Gepreel M.A.H., Niinomi M. Biocompatibility of Ti-alloys for long-term implantation. *Journal of the Mechanical Behavior of Biomedical Materials*, 2013, vol. 20, pp. 407–415. DOI: 10.1016/j.jmbbm.2012.11.014.

3. Sánchez-López J.C., Rodríguez-Albelo M., Sánchez-Pérez M., Godinho V., López-Santos C., Torres Y. Ti6Al4V coatings on titanium samples by sputtering techniques: Microstructural and mechanical characterization. *Journal of Alloys and Compounds*, 2023, vol. 952, p. 170018. DOI: 10.1016/j.jallcom.2023.170018.

4. Banerjee R., Das S., Mukhopadhyay K., Nag S., Chakrabortty A., Chaudhuri K. Involvement of in vivo induced cheY-4 gene of Vibrio cholerae in motility, early adherence to intestinal epithelial cells and regulation of virulence factors. *FEBS Letters*, 2002, vol. 532, pp. 221–226. DOI: 10.1016/S0014-5793(02)03678-5.

5. Olmedo D., Fernández M.M., Guglielmotti M.B., Cabrini R.L. Macrophages related to dental implant failure. *Implant Dentistry*, 2003, vol. 12, pp. 75–80. DOI: 10.1097/01.ID.0000041425.36813.A9.

6. Zhao L., Chu P.K., Zhang Y., Wu Z. Antibacterial coatings on titanium implants. *Journal of Biomedical Materials Research. Part B: Applied Biomaterials*, 2009, vol. 91, pp. 470–480. DOI: 10.1002/jbm.b.31463.

7. Tian J., Xu K., Hu J., Zhang S., Cao G., Shao G. Durable self-polishing antifouling Cu-Ti coating by a micron-scale Cu/Ti laminated microstructure design. *Journal of Materials Science & Technology,* 2021, vol. 79, pp. 62–74. DOI: 10.1016/j.jmst.2020.11.038.

8. Zhang J.Q., Cao S., Liu Y., Bao M.M., Ren J., Li S.Y., Wang J.J. Tribocorrosion behavior of antibacterial Ti–Cu sintered alloys in simulated biological environments. *Rare Metals*, 2022, vol. 41, pp. 1921–1932. DOI: 10.1007/s12598-021-01943-6.

9. Adamiak B., Wiatrowski A., Domaradzki J., Kaczmarek D., Wojcieszak D., Mazur M. Preparation of multicomponent thin films by magnetron co-sputtering method: The Cu-Ti case study. *Vacuum*, 2019, vol. 161, pp. 419–428. DOI: 10.1016/j.vacuum.2019.01.012.

10. Jin X., Gao L., Liu E., Yu F., Shu X., Wang H. Microstructure, corrosion and tribological and antibacterial properties of Ti–Cu coated stainless steel. *Journal of the Mechanical Behavior of Biomedical Materials*, 2015, vol. 50, pp. 23–32. DOI: 10.1016/j.jmbbm.2015.06.004.

11. Wojcieszak D., Kaczmarek D., Antosiak A., Mazur M., Rybak Z., Rusak A., Szponar B. Influence of Cu–Ti thin film surface properties on antimicrobial activity and viability of living cells. *Materials Science and Engineering: C*, 2015, vol. 56, pp. 48–56. DOI: 10.1016/j.msec.2015.06.013.

12. Zhu Y., Yan M., Zhang Q., Wang Q., Zhuo H. Effects of the prefabricated Cu-Ti film on the microstructure and mechanical properties of the multiphase coating by thermo plasma nitriding on C17200 Cu alloy. *Coatings*, 2019, vol. 9, p. 694. DOI: 10.3390/coatings9110694.

13. Wang Z.Q., Wang X.R. Microstructure and flame-retardant properties of Ti-Cu coating on Tc11 prepared via electrospark deposition. *Material Engineering and Mechanical Engineering: Proceedings of Material Engineering and Mechanical Engineering (MEES 2015)*. World Scientific, 2016, pp. 1283–1291. DOI: 10.1142/9789814759687_0144.

14. Radek N. Experimental investigations of the Cu-Mo and Cu-Ti electro-spark coatings modified by laser beam. *Advances in Manufacturing Science and Technology*, 2008, vol. 32, pp. 53–68.

15. Kayali Yu., Yalçin M.C., Buyuksagis A. Effect of electro spark deposition coatings on surface hardness and corrosion resistance of ductile iron. *Canadian Metallurgical Quarterly*, 2023, vol. 62, pp. 483–496. DOI: 10.1080/00084433.2022.2119039.

16. Zhao H., Gao Ch., Guo Ch., Xu B., Wu X.Yu., Lei J.G. In-situ TIC-reinforced NI-based composite coatings fabricated by ultrasonic-assisted electrospark powder deposition. *Journal of Asian Ceramic Societies*, 2023, vol. 11, pp. 26–38. DOI: 10.1080/21870764.2022.2142368.

17. Burkov A.A., Pyachin S.A. Formation of WC–Co coating by a novel technique of electrospark granules deposition. *Materials & Design*, 2015, vol. 80, pp. 109–115. DOI: 10.1016/j.matdes.2015.05.008.

18. Burkov A.A. Production amorphous coatings by electrospark treatment of steel 1035 in a mixture of iron granules with CrMoWCBSi powder. *Obrabotka metallov (tekhnologiya, oborudovanie, instrumenty) = Metal Working and Material Science*, 2019, vol. 21, no. 4, pp. 19–30. DOI: 10.17212/1994-6309-2019-21.4-19-30. (In Russian).

19. Burkov A.A., Kulik M.A. Wear-resistant and anticorrosive coatings based on chrome carbide Cr7C3 obtained by electric spark deposition. *Protection of Metals and Physical Chemistry of Surfaces*, 2020, vol. 56, pp. 1217–1221. DOI: 10.1134/S2070205120060064.

20. Burkov A.A. One-stage deposition of Ti–Cu coatings by electric spark treatment of Ti6Al4V titanium alloy with an anode of copper and titanium granules. *Fundamental'nye problemy sovremennogo materialovedenia = Basic Problems of Material Science (BPMS)*, 2023, vol. 20, pp. 372–380. DOI: 10.25712/ASTU.1811-1416.2023.03.010. (In Russian).

21. Burkov A.A., Chigrin P.G., Dvornik M.I. Electrospark CuTi coatings on titanium alloy Ti6Al4V: corrosion and wear properties. *Surface and Coatings Technology*, 2023, vol. 469, p. 129796. DOI: 10.1016/j.surfcoat.2023.129796.

22. Durdu S., Usta M., Berkem A.S. Bioactive coatings on Ti6Al4V alloy formed by plasma electrolytic oxidation. *Surface and Coatings Technology*, 2016, vol. 301, pp. 85–93. DOI: 10.1016/j.surfcoat.2023.129796.

23. Jamnapara N.I., Frangini S., Alphonsa J., Chauhan N.L., Mukherjee S. Comparative analysis of insulating properties of plasma and thermally grown alumina films on electrospark aluminide coated 9Cr steels. *Surface and Coatings Technology*, 2015, vol. 266, pp. 146–150. DOI: 10.1016/j.surfcoat.2015.02.028.

24. Campo K.N., de Lima D.D., Lopes É.S.N., Caram R. On the selection of Ti–Cu alloys for thixoforming processes: phase diagram and microstructural evaluation. *Journal of Materials Science*, 2015, vol. 50, pp. 8007–8017. DOI: 10.1007/s10853-015-9367-4.

25. Fan Y., Fan J., Wang C. Formation of typical Ti–Cu intermetallic phases via a liquid-solid reaction approach. *Intermetallics*, 2019, vol. 113, p. 106577. DOI: 10.1016/j.intermet.2019.106577.

26. Bohórquez C.D., Pérez S.P., Sarmiento A., Mendoza M.E. Effect of temperature on morphology and wear of a Cu-Ti-TiC MMC sintered by abnormal glow discharge. *Materials Research Express*, 2020, vol. 7, p. 026501. DOI: 10.1088/2053-1591/ab6e3b.

27. Modestov A.D., Zhou G.D., Wu Y.P., Notoya T., Schweinsberg D.P. A study of the electrochemical formation of Cu(I)-BTA films on copper electrodes and the mechanism of copper corrosion inhibition in aqueous chloride/benzotriazole solutions. *Corrosion Science*, 1994, vol. 36, pp. 1931–1946. DOI: 10.1016/0010-938X(94)90028-0.

28. Rosalbino F., Scavino G. Corrosion behaviour assessment of cast and HIPed Stellite 6 alloy in a chloride-containing environment. *Electrochimica Acta*, 2013, vol. 111, pp. 656–662. DOI: 10.1016/j.electacta.2013.08.019.

29. Ding Y., Kong L., Lei W., Li Q., Ding K., He Y. Study on the technology of surface strengthening Ti–6Al–4V alloy by near-dry multi-flow channel electrode electrical discharge machining. *Journal of Materials Research and Technology*, 2024, vol. 28, pp. 2219–2234. DOI: 10.1016/j.jmrt.2023.12.133.

30. Guo S., Lu Y., Wu S., Liu L., He M., Zhao C., Lin J. Preliminary study on the corrosion resistance, antibacterial activity and cytotoxicity of selective-laser-melted Ti6Al4V-xCu alloys. *Materials Science and Engineering: C*, 2017, vol. 72, pp. 631–640. DOI: 10.1016/j.msec.2016.11.126.

31. Alves A.C., Wenger F., Ponthiaux P., Celis J.P., Pinto A.M., Rocha L.A., Fernandes J.C.S. Corrosion mechanisms in titanium oxide-based films produced by anodic treatment. *Electrochimica Acta,* 2017, vol. 234, pp. 16–27. DOI: 10.1016/j.electacta.2017.03.011.

32. Cao S., Zhang Z.M., Zhang J.Q., Wang R.X., Wang X.Y., Yang L., Zhang E.L. Improvement in antibacterial ability and cell cytotoxicity of Ti–Cu alloy by anodic oxidation. *Rare Metals*, 2022, vol. 41, pp. 594–609. DOI: 10.1007/s12598-021-01806-0.

33. Lu M., Zhang Z., Zhang J., Wang X., Qin G., Zhang E. Enhanced antibacterial activity of Ti-Cu alloy by selective acid etching. *Surface and Coatings Technology*, 2021, vol. 421, p. 127478. DOI: 10.1016/j.surfcoat.2021.127478.

34. *Guidelines for drinking-water quality*. World Health Organization, 2002.

35. Ren L., Yang K. Antibacterial design for metal implants. *Metallic Foam Bone.* Woodhead Publishing, 2017, pp. 203–216. DOI: 10.1016/B978-0-08-101289-5.00008-1.

36. Kaplan Y., Işıtan A. Tribological behavior of borided Ti6Al4V alloy under simulated body fluid conditions. *Acta Physica Polonica A*, 2018, vol. 134, pp. 271–274. DOI: 10.12693/APhysPolA.134.271.

37. Shao J.Z., Li J., Song R., Bai L.L., Chen J.L., Qu C.C. Microstructure and wear behaviors of TiB/TiC reinforced Ti2Ni/a(Ti) matrix coating produced by laser cladding. *Rare Metals*, 2020, vol. 39, pp. 304–31. DOI: 10.1007/s12598-016-0787-3.

Conflicts of Interest

The authors declare no conflict of interest.